Available online at www.sciencedirect.com
ScienceDirect
Ceramics International 37 (2011) 363–368
CERAMICS INTERNATIONAL
www.elsevier.com/locate/ceramint

Testing method to assess lifetime of EB-PVD thermal barrier coatings on tubular specimens in static and cyclic oxidation tests

R.W. Steinbrech, V. Postolenko, J. Mönch, J. Malzbender *, L. Singheiser

Forschungszentrum Jülich GmbH, IEF-2, 52425 Jülich, Germany

Received 17 June 2010; received in revised form 18 July 2010; accepted 1 September 2010
Available online 29 September 2010

Abstract

A testing methodology is presented to assess the delamination failure of an yttria stabilized zirconia electron beam physical vapor deposited (EB-PVD) top-coat as studied for tubular specimens applying short thermal cycles with high heating and cooling rates as well as for oxidation tests at constant temperature. The influence of maximum temperature and specimen diameter were investigated. Higher maximum temperatures as well as a smaller specimen diameter resulted in shorter lifetimes. No significant difference was observed between the static and cyclic oxidation tests. The failure relevant time at elevated temperatures is correlated with the thickness of the thermally growing oxide (TGO) scale developing on the bond coat. The experimental results can be described using a residual stress based analytical approach. In the model the lifetime is assumed to be terminated when a critical stress is reached.

Keywords: Mechanical testing; Delamination; Lifetime; Fracture; Thermal cycling; Thermal barrier coatings (TBC)

1. Introduction

The direction of gas turbine development for power generation and aero-engine application aims towards an increase in efficiency. Materials development is focused on the turbine blades and vanes, especially of the first turbine stage. These components must withstand in addition to mechanical loads also high temperature exposure and oxidizing environments. Due to the required mechanical properties, e.g. high strength up to 1000 °C and resistance against high temperature inelastic deformation, nickel-based super alloys are widely used as structural base material in this turbine part.

In order to protect the base material against high temperature oxidation, two types of metallic coatings are usually applied, which are known to form dense protective oxide scales: (i) aluminides or Pt-modified aluminide coatings normally applied by pack cementation or chemical vapor deposition (CVD) [1] and (ii) NiCoCrAlY, CoCrAlY, NiCrAlY—layers are normally coated by vacuum plasma spraying (VPS), low pressure plasma spraying (LPPS) [2] or high velocity oxyfuel spraying (HVOF) [3]. On top of this protection layer the ceramic thermal barrier coating (TBC) is deposited. Yttria stabilized zirconia as standard TBC material is conventionally applied either by electron beam physical vapor deposition (EB-PVD) [4] or by air plasma spraying (APS) [5]. In combination with internal component cooling the TBCs develop a thermal gradient which protects the metals beneath and ultimately increases the efficiency of the gas turbine.

Thermal barrier coating systems are currently not operated in closely to the limits of their mechanical integrity since the possible failure mechanisms are not yet fully understood and thus the temperature dependent lifetime of the coating system cannot be predicted with sufficient reliability. However, the demand for higher efficiency of gas turbines requires a predictability of the TBC failure that terminates the lifetime. Among the parameters which have impact on the failure are residual stresses due to the deposition process of the coatings, thermal stresses due to the difference in thermal expansion coefficients between metallic substrate/bond coat and ceramic top-coat and residual stresses due to the bond coat oxidation processess, e.g. thermally grown oxide (TGO) formation [6]. Tensile stresses can cause cracks to nucleate and propagate as the system experiences thermal cycling [6–10]. Eventually, the cracks might coalesce causing the TBC to buckle and

* Corresponding author. Tel.: +49 2461616964; fax: +49 2461613699.
E-mail address: j.malzbender@fz-juelich.de (J. Malzbender).

0272-8842/$36.00
doi:10.1016/j.ceramint.2010.09.028

eventually to spall [6,8,11,12]. Furthermore, in service also the applied mechanical loads contribute to the stress state. Although many factors control TBC failure, thermally grown oxide (TGO) development and subsequent thickening is generally considered to be most important [13].

Very detailed investigations have been carried out for systems comprising EB-PVD thermal barrier coatings [6–9,14–20]. Depending on the bond coat composition the TGO develops either displacement instabilities associated with the elongation of the TGO since it deforms into the relative soft bond coat yielding cracks form in the TBC above the intrusion [12,16] or the TGO develops thickness heterogeneities (often referred to as ''pegs''), which contain oxides other than alumina, e.g. yttrium aluminum garnet (YAG) [17,21]. Contrary to the Pt–aluminide system, for NiCoCrAlY bond coats delamination occurs primarily along the interface between the TGO and the bond coat [18–21]. The cracks extend through the TGO only at the ''pegs'' locations and do not enter into the TBC layer. In contrast to the Pt–aluminide system, the durability of the NiCoCrAlY system appears to be invariant of the cycle time [18], the TGO thickness at failure is essentially the same under cyclic and isothermal conditions.

Approaches to predict the limit of mechanical integrity of the TBCs have generally concentrated on models based on empirical/phenomenological fatigue life relationships. The lifetime of the TBC is correlated with the accumulated damage due to mechanical straining and oxidation [22]. It has been argued that slow sub-critical growth determines the lifetime in TBC systems. However, the conditions under which this could occur have received only limited attention [23].

In the literature, several approaches for stress analysis and lifetime prediction of TBC systems are reported [24–28]. Qualitative strategies for the optimization of TBC systems might be based on the results obtained using finite element (FEM) simulations. Based on global fracture mechanics data of the EB-PVD TBC and the TBC/BC interface, Evans et al. developed a systematic mapping of the influence of thickness and stiffness [6] as well as of thermal gradients [29] on the failure mode and lifetime. A model based on thermal misfit strains and TGO growth strain based model was developed within a NASA project [30]. Oechsner [31] proposed a lifetime prediction method based on a combination of fracture mechanics and micromechanics. Renusch et al. [32] developed a two step model based on a critical strain approach that takes into account subsequent delamination and segmentation cracking of plasma-sprayed TBCs. Busso et al. [23] predicted the lifetime of EB-PVD TBCs using stress analyses by elastic–viscoplastic FEM, statistical approaches describing the TBC/bond coat interface morphology and TGO growth combined with damage accumulation based on experimental delamination crack propagation data. A recently developed semi-empirical model for cyclic oxidation correlates the initial crack growth with the TGO thickness development and calculates the subsequent propagation of longer crack using a fracture mechanics approach [33].

The present work develops a simplified analytical lifetime model for EB-PVD and furthermore extends TBC failure prediction to coatings on curved specimens. First, experimental results are presented which have been obtained from fast thermal cycle and static oxidation tests with tubular specimens. Then a model is derived which describes the measured lifetimes as a function of maximum temperature and surface curvature including reasonable physical assumptions about the temperature and time dependent TGO growth. Microstructural verification was not possible due to proprietary interests of the coatings supplier.

2. Experimental procedure

2.1. Materials

Tubular specimens of the Ni-base super alloy CMSX-4 substrate coated on the outer surface of the cylindrical specimens with a proprietary Pt-based bond coat (10 μm) and yttria stabilized zirconia as top coat (150 μm) were provided by Rolls Royce Deutschland, Berlin. Three different diameters (6, 12 and 19 mm) of the tubular multilayer specimens had been supplied. All specimens had a substrate thickness of ∼1 mm and a length of 30 mm.

2.2. Oxidation experiments

Isothermal (33 specimens) and short-cycle oxidation (19 specimens) was carried out with a specially designed heating and cooling set-up. No additional temperature gradient was applied during the annealing at elevated temperature. The system comprised as main components a vertically movable furnace (XERION, Freiberg, Germany) with an internal specimen tray and a stationary vertical quartz tube with a stage for single specimen positioning (Fig. 1). For cyclic oxidation the specimen was mounted and fixed in the stage on top of the quartz tube. The set-up allowed rapid internal air-cooling that was applied in the case of the cyclic tests. In addition, during the cooling sequences of the cyclic tests the surface of the EB-PVD top coat could be observed using a long distance microscope system (Questar, QM 100, USA). The specimens temperature was controlled by a thermocouple, welded to the CMSX-4 substrate of the tubes.

The samples were annealed up to different maximum temperatures between $1030 \leq T_{max} \leq 1130\ ^{\circ}C$ in laboratory air. Each specimen was annealed separately; hence failure detection was possible for thermally cycled and isothermally annealed specimens. In case of the cyclic oxidation, fast heating/cooling sequences (up to 15 K/s, approximately 2 min for heating to maximum temperature and cooling, respectively) were applied with 5 min dwell-time at T_{max} (Fig. 2). In the cyclic oxidation tests the time to TBC failure could be determined with the accuracy of one cycle. In the case of the isothermal tests the heating rate was 20 K/min, the cooling to RT took place within approximately 5 min after the specimens were taken out of the furnace. During isothermal oxidation interrupted tests helped to approach the limit of mechanical integrity by visual inspection (see below). The lifetime of the TBC system was defined in both cases as the time accumulated at high temperature before the failure. Due to proprietary

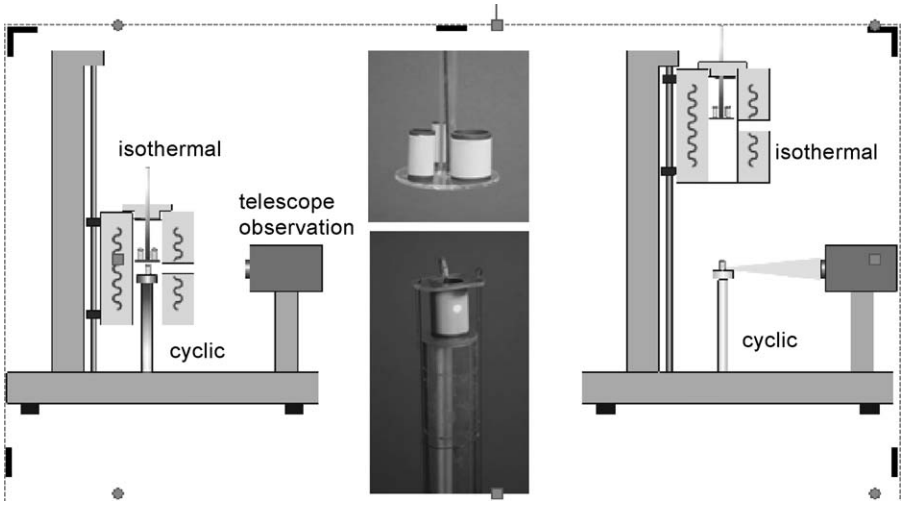

Fig. 1. Combined static and cyclic oxidation tests with tubular specimens.

restrictions only normalized lifetimes are given in the following sections.

The end of the mechanical integrity was derived by a combination of different methods. Parts of the results were obtained from interrupted tests with a visual inspection at room temperature. For example, a specimen with a diameter of 6 mm was oxidized at 1030 °C and showed no evidence of failure after different times, except the last step where complete delamination occurred. Defining the accumulated time at high temperatures as failure time the other examinations could be attributed to 61, 80 and 93% of the lifetime. Alternatively, different samples of identical size were exposed to different pre-defined times and temperature and the difference in time between surviving and delaminating TBCs was used to extract a minimum lifetime. In some cases preferentially with specimens of 19 mm diameter, the oxidation time was not long enough to cause TBC failure. Thus, the longest exposure time was used as a conservative estimate of the lifetime.

In cyclic oxidation tests the time to TBC failure could be determined in principle within the accuracy of one cycle. However, also some delayed failure at RT was observed where the minimum waiting time was approximately 20 h. Besides this possible reduction in cyclic lifetime again a conservative estimate had to be used when specimens did not reveal TBC failure within the experimental time available for cyclic oxidation at lower maximum temperatures.

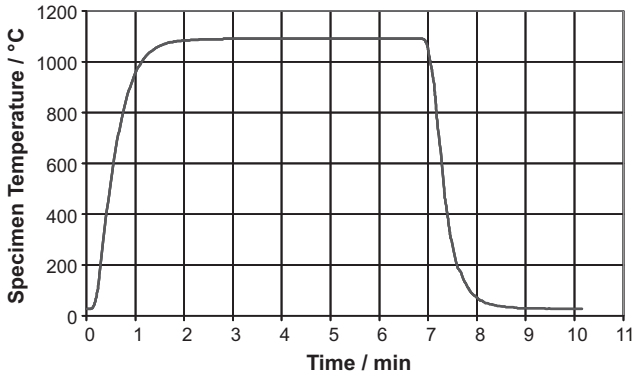

Fig. 2. Temperature scheme in cyclic oxidation tests.

3. Results and discussion

3.1. Isothermal oxidation

Although the number of specimens was limited the outlined approach turned out to give a good description of the effect of the specimen geometry and time at elevated temperature on the lifetime. The analysis was further complicated by slow crack growth at RT.

Typical specimens of different diameter, all oxidized isothermally at 1100 °C are shown in Fig. 3. Immediately after removal from the furnace a lateral macro-crack could be observed near the rim of the TBC on the 6 mm specimen. This crack continued to grow parallel to the specimen axis and, already after 7 min the TBC was completely delaminated. In the 12 mm specimen a visible initial macroscopic delamination of the ceramic top coat was detected after approximately 30 min at RT, whereas the 19 mm sample revealed a first delamination of the TBC after 7 h. Longer exposures at RT resulted only in minor progress of the delamination. Fig. 3 shows macro-pictures of the three specimens after 70 h at RT in air.

The time of delayed macroscopic failure at RT was not incorporated into the analysis to simplify the lifetime parameter

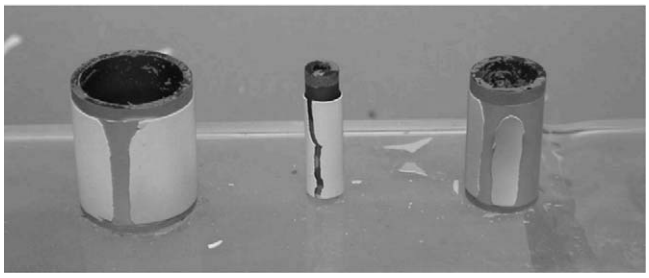

Fig. 3. Delamination of EB-PVD coatings. Spallation pattern after isothermal oxidation at 1100 °C.

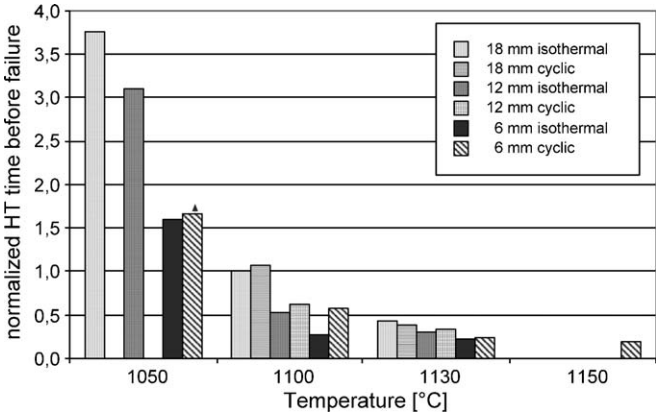

Fig. 4. Normalized lifetime of EB-PVD coated tubular samples in isothermal oxidation and cyclic oxidation tests.

determination. In Fig. 4 only the time at maximum temperature before the failure at RT is plotted. Note that the lifetime is normalized. The isothermal oxidation data consider the different maximum temperatures and the three tube diameters. It can be seen that the lifetime of the TBC system strongly depends on the maximum exposure temperature. Comparing for example tubes of 12 mm diameter, the 1130 °C specimen has a lifetime, which is more than an order of magnitude shorter than the lifetime of the specimen exposed at 1050 °C. There is in addition a clear dependence of the lifetime on the specimen diameter. A smaller tube diameter results in decrease of the lifetime by more than a factor of two for a maximum temperature of 1050 °C.

3.2. Cyclic oxidation

The first visible macroscopic delamination of the ceramic coating was in almost all cases observed at room temperature. Again a delayed failure was observed, qualitatively correlated with the specimen diameter. A larger diameter caused a longer delay. In order to monitor the failure delay time at RT, the specimens were fixed on the mounting stage of the quartz tube. This eliminates possible mechanical damage due to handling. Considering the uncertain location of the first failure, 360° coverage of the specimen surface was achieved by using two inclined mirrors behind the specimen. A digital camera system recorded all visible changes on the coating surface.

The lifetime of the EB-PVD specimens exposed to cyclic oxidation is also displayed in Fig. 4 as a function of maximum temperature and different diameter. Again a clear dependence of the time-to-failure on the specimen geometry, e.g. specimen diameter, as well as on the maximal temperature is given. The TBC on the tubes with the smallest diameter (6 mm) failed first and furthermore, the shortest lifetime was observed for the specimens exposed to the highest temperature (1130 °C).

3.3. Comparison of isothermal and cyclic oxidation results

A comparison of the cyclic and static oxidation results in Fig. 4 reveals that the applied short oxidation cycles have neither a significant nor a negative influence on the EB-PVD lifetime. If at all, time at temperature for the chosen short cycle condition appears to be slightly longer before macroscopic delamination occurs. Also the pronounced influence of specimen diameter on the lifetime is similar in both cases.

3.4. Lifetime prediction

The subsequent model describes the macroscopic lifetime results based on a simplified analytical relationship, which neglects the observed ''desktop'' effect leading to the delayed TBC delamination at RT. Due to proprietary reasons, details on the microstructural failure mechanisms did not enter into the approach. However, the basic correlation of TBC delamination with TGO development, which has been implemented in most TBC failure models, is included.

The model starts with the assumption that TBC failure (radial fracture, delamination) occurs, when the critical radial stress intensity (K_{radial}) is exceeded at the TGO/bond coat interface. In the absence of additionally applied radial stresses only the thermal mismatch and oxidation induced stresses contribute to the stress intensity. Since complementary fluorescence spectroscopic investigations of the lateral mismatch stresses did not reveal major changes in TGO stress versus exposure time [34], the modeling approach was further simplified considering only the development of the radial residual stress intensity (K_{res}). If furthermore, and following the same argument, interfacial crack growth [35] is neglected as a parameter which influences K_{res} before the ultimate TBC delamination, the modeling approach reduces to an evaluation of the residual radial stress (σ_{res}^{radial}).

The radial stress of the multilayer thermal barrier system is generally a function of different thermo-mechanical properties and geometrical features (e.g. thermal expansion coefficients α_i, Youngs moduli E_i, thickness of the layers d_i, radius of tube curvature r^m and temperature) [36,37]. Note that due to high temperature stress relaxation the ductile-to-brittle transition temperature $\Delta T_{DBTT-RT}$ needs to be considered:

$$\sigma_c^{radial} = f(d^i, E^i, \alpha^i, d^{TGO}, 1/r^m, \Delta T_{DBTT-RT}) \quad (1)$$

Index i refers to the layers of the TBC system. The thickness of the thermally grown oxide d^{TGO} changes with time. Considering simulations results [38] the residual stress in the interface appears to increase rather linear with TGO thickness after an initial non-linear increase for small TGO thicknesses. In relationship (1) the parameters which do not significantly change during the oxidation tests can be joined to a constant parameter A to obtain a simplified equation leaving only TGO thickness and specimen radius as variables:

$$\sigma_c^{radial} = A \cdot \frac{d_c^{TGO}}{r^m} \quad (2)$$

The growth of the TGO thickness can be expressed by:

$$d_c^{TGO} = k \cdot t^n = C \cdot \exp\left(-\frac{Q}{RT}\right) \cdot t^n \quad (3)$$

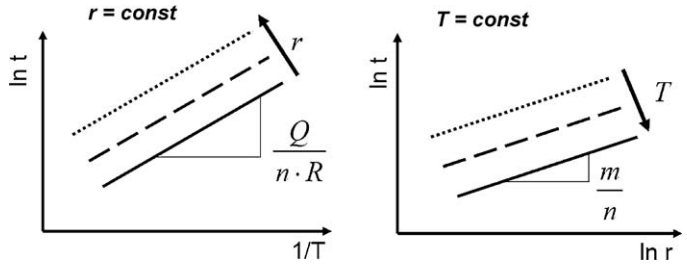

Fig. 5. Lifetime of EB-PVD TBCs as a function of temperature and specimen radius.

where t is the oxidation time, k – the oxidation rate constant, n – the oxidation rate exponent [39], Q – the activation energy of the TGO growth, R – the universal gas constant and C a pre-factor. Yielding for the critical radial stress:

$$\sigma_c^{radial} = A \cdot r^{-m} \cdot C \cdot \exp\left(-\frac{Q}{RT}\right) \cdot t^n \quad (4)$$

Note that for the same critical stress and a constant tube radius the TGO thickness at failure should be identical for different maximum oxidation temperatures since the temperature dependence of the critical failure stress can be neglected. Eq. (4) allows a straight forward comparison with the experimental results obtained from the oxidation experiments. Logarithmic notation and re-arrangement with respect to the (accumulated) oxidation time yields:

$$\ln t = \frac{Q}{n \cdot R} \cdot \frac{1}{T} + \frac{m}{n} \ln r + \frac{1}{n}(\ln \sigma_c^{radial} - \ln C - \ln A) \quad (5)$$

In case of TBC failure the parameter t provides a direct measure of the lifetime. Note that for the specimens with the same geometry, i.e. radius, a shorter lifetime is expected at higher oxidation temperatures. To examine the validity of the present analytical approach it is important to describe all results with a single set of parameters. The use of Eq. (5) is supported by the fact that the pressure perpendicular to a coatings interface for tubular specimens scales linear with the specimen radius in a log–log representation [40].

In graphical representations of Eq. (5) the experimentally determined lifetime of the TBC can be plotted either as a function of inverse temperature or specimen radius (Fig. 5). The slope in the $\ln t - 1/T$ diagram is $Q/(n{\cdot}R)$, if the third term in Eq. (5) is constant. Similarly at a given maximum temperature the specimens with smaller radius should have a shorter lifetime. The lower the oxidation temperature the longer is the expected lifetime. The slope of $\ln t - \ln r$ curves permits a determination of the ratio m/n.

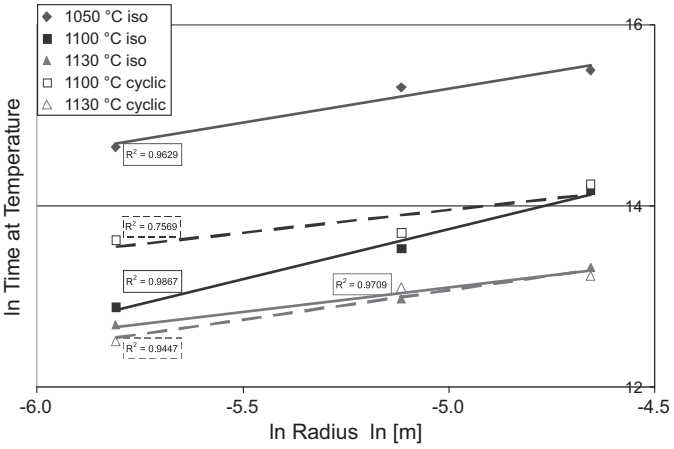

Fig. 7. Lifetime of EB-PVD TBCs on tubular specimens as a function of specimen radius.

The experimental results obtained from the isothermal and cyclic oxidation tests of the EB-PVD coated tubular specimens are plotted in Fig. 6. The data can be described by the derived relationship. The plot reveals no major difference between the isothermal and the cyclic oxidation tests. The slope in the $\ln t - 1/T$ plot is approximately the same for the specimens with different tube radius. From the slope the pre-factor of the temperature term is determined as $Q/(n \cdot R) \approx 53,300$.

The activation energy Q for TGO growth, calculated from an Arrhenius plot of the parabolic growth constants, is reported to be 139 kJ/mol [41]. Thus a TGO growth exponent of $n \approx 0.3$ can be estimated for specimens with the same radius, a reasonable value for an alumina TGO scale.

Fig. 7 shows the dependence of the lifetime on the tube radius for both isothermal and cyclic oxidation experiments. Again, no significant difference is observed between the isothermal and cyclic loading modes. The experimental data

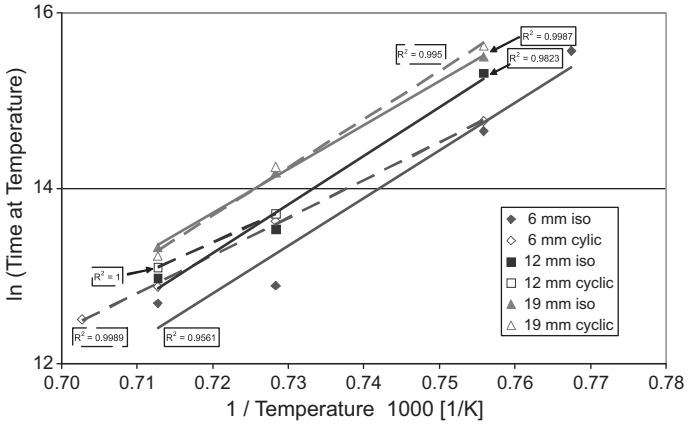

Fig. 6. Lifetime of EB-PVD TBCs on tubular specimens as a function of inverse temperature.

can be fitted to curves which have approximately the same slope: $m/n \approx 0.67$. Using the above determined TGO growth exponent of $n \approx 0.3$ the contribution of the specimen radius to lifetime follows a power law with the exponent $m \approx 0.2$.

4. Conclusions

Higher maximum temperatures as well as a smaller specimen diameter resulted in shorter lifetimes. No significant difference was observed between the static and cyclic oxidation tests. The failure relevant time at elevated temperatures is correlates with the TGO thickness. In a logarithmic representation the lifetimes appears to be linear proportional to the inverse temperature and the specimen diameter. The lifetime results, obtained from isothermal and cyclic oxidation experiments of the EB-PVD TBC specimens with different geometry and various maximum oxidation temperatures were successfully described using an analytical model, based on a critical radial stress concept. In the model the lifetime is assumed to be terminated when a critical stress is reached.

Although the experimental results are limited for TBC coatings of a thickness of 150 μm on CMSX-4 substrates they provide a good basis for the understanding of the effect of the curvature on the delamination failure during isothermal and cyclic oxidation. Future development should aim at a consideration of slow crack growth at RT and extending the lifetime description to consider statistical effects. From a practical point of view the model permits a consideration of the local curvature variations of blades and vanes. An analytical basis is given to extent lifetime prediction towards decreasing temperature and curvature.

Acknowledgements

The authors gratefully acknowledge the support from and the stimulating discussion with Dr. J. Xu, Rolls Royce Deutschland (RRD). Furthermore, the time and efforts spend in assisting the development of the highly sophisticated thermal cycling set-up by T. Osipova has to be emphasized. The work was funded as part of the TBC project ''MARCKO'' by the German Ministry of Economics and Technology.

References

[1] S.A.K. Sinha, ASM Handbook 4 (1991) 437.
[2] D. Wortman, B.A. Nagaraj, E.C. Duderstadt, Mater. Sci. Eng. A120–121 (1989) 433.
[3] J.R. Nicholls, JOM 52 (2000) 28.
[4] O. Unal, T.E. Mitchell, A.H. Heuer, J. Am. Ceram. Soc. 77 (1994) 984.
[5] R.A. Miller, J. Thermal. Spray Technol. 6 (1997) 35.
[6] A.G. Evans, D.R. Mumm, J.W. Hutchinson, G.H. Meier, F.S. Pettit, Prog. Mater. Sci. 46 (2001) 505.
[7] J.A. Ruud, A. Bartz, M.P. Borom, C.A. Johnson, J. Am. Ceram. Soc. 84 (2001) 1545.
[8] D.R. Mumm, A.G. Evans, I.T. Spitsberg, Acta Mater. 49 (2001) 2329.
[9] J.M. Ambrico, M.R. Begley, E.H. Jordan, Acta Mater. 49 (2001) 1577.
[10] A.M. Karlsson, J.W. Hutchinson, A.G. Evans, J. Mech. Phys. Solids 50 (2002) 1565.
[11] S.R. Choi, J.W. Hutchinson, A.G. Evans, Mech. Mater. 31 (1999) 431.
[12] T. Xu, M.Y. He, A.G. Evans, Acta Mater. 51 (2003) 3807.
[13] T. Xu, S. Faulhaber, C. Mercer, M. Maloney, A.G. Evans, Acta Mater. 52 (2004) 1439.
[14] M.J. Stigere, N.M. Yanar, M.G. Toppings, F.S. Pettit, G.H. Meier, Z. Metallkunde 90 (1999) 1069.
[15] P.K. Wright, Mater. Sci. Eng. A245 (1998) 191.
[16] I.T. Spitsberg, D.R. Mumm, A.G. Evans, Mater. Sci. Eng. A394 (2005) 176.
[17] G.M. Kim, N.M. Yanar, E.N. Hewitt, F.S. Pettit, G.H. Meier, Scr. Mater. 46 (2002) 489.
[18] N.M. Yanar, G.H. Meier, F.S. Pettit, Scr. Mater. 46 (2002) 325.
[19] Y.H. Sohn, J.H. Kim, E.H. Jordan, M. Gell, Surf. Coat. Technol. 146–147 (2001) 70.
[20] D. Strauss, G. Muller, G. Schumacher, V. Engelko, W. Stamm, D. Clemens, W.J. Quaddakers, Surf. Coat. Technol. 135 (2001) 196.
[21] D.R. Mumm, A.G. Evans, Acta Mater. 48 (2000) (1815).
[22] N.P. Padture, M. Gell, E.H. Jordan, Science 296 (2002) 280.
[23] E.P. Busso, L. Wright, H.E. Evans, L.N. McCartney, S.R.J. Saunders, S. Osgerby, J. Nunn, Acta Mater. 55 (2007) 1491.
[24] A.M. Freborg, B.L. Ferguson, W.J. Brindley, G.J. Petrus, Mater. Sci. Eng. A245 (1998) 182.
[25] M. Ahrens, R. Vaβen, D. Stöver, Surf. Coat. Technol. 161 (2002) 26.
[26] K. Sfar, J. Aktaa, D. Munz, Mater. Sci. Eng. A333 (2002) 351.
[27] J. Rösler, M. Bäker, K. Aufzug, Acta Mater. 52 (2004) 4809.
[28] M. Bäker, J. Rösler, G. Heinze, Acta Mater. 53 (2005) 469.
[29] A.G. Evans, J.W. Hutchinson, Surf. Coat. Technol. 201 (2007) 7905.
[30] S.M. Meier, D.M. Nissey, K.D. Sheffler, T.A. Cruse, J. Eng. Gas Turbine Power 114 (1992) 258.
[31] M. Oechsner, VDI Fortschrittsberichte 263 (2001).
[32] D. Renusch, H. Echsler, M. Schütze, Mater. High Temp. 21 (2004) 77.
[33] T. Beck, R. Herzog, O. Trunova, M. Offermann, R.W. Steinbrech, L. Singheiser, Surf. Coat. Technol. 202 (2008) 5901.
[34] J. Toscano, Ph.D. Thesis, RWTH Aachen, Germany, 2008.
[35] J. Malzbender, I. Escobar, R. Herzog, R.W. Steinbrech, H. Öttel, Ceram. Eng. Sci. Proc. 26/3 (2005) 55.
[36] J. Malzbender, J.M.J. den Toonder, A.R. Balkenende, G. de With, Mater. Sci. Eng. Rep. 36 (2002) 47.
[37] J. Malzbender, R.W. Steinbrech, J. Mater. Res. 18 (2003) 1374.
[38] C.-H. Hsueh, E.R. Fuller, Mater. Sci. Eng. A 283 (2000) 46.
[39] W.J. Quadakkers, Werkst. Korros. 41 (1990) 659.
[40] X.C. Zhang, B.S. Xu, H.D. Wang, Y. Jiang, Y.X. Wu, Com. Sci. Technol. 66 (2006) 2249.
[41] S. Sridharan, L. Xie, E.H. Jordan, M. Gell, K.S. Murphy, Mater. Sci. Eng. A393 (2005) 51.